rinted in U.S.A.

Paper No.
75-WA/Aut-26

an ASME
publication

W. J. BOOK
Assistant Professor of Mechanical Engineering, Georgia Institute of Technology, Atlanta, Ga.

O. MAIZZA-NETO
Assistant Professor of Mechanical Engineering, Escola Politecnia da U.S.P., Sao Paulo, S. P., Brazil

D. E. WHITNEY
Section Chief, Charles Stark Draper Lab., Cambridge, Mass.

Feedback Control of Two Beam, Two Joint Systems With Distributed Flexibility[1]

The control of the flexible motion in a plane of two pinned beams is addressed with application to remote manipulators. Three types of linear feedback control schemes are considered: joint angle and velocity feedback with (GRC) and without (IJC) cross joint feedback, and feedback of flexible state variables (FFC). Two models of the distributed flexibility are presented along with some results obtained from them. The relative merit of the three control schemes is discussed.

Introduction

Manipulators are found in industrial and research environments which are too hazardous or unpleasant for a human worker. Requirements for safety and improved working conditions are becoming more stringent due to legislation and collective bargaining, while international competition requires that ever higher productivity be achieved. Computer commanded industrial manipulators can potentially meet the increased demands of both worker safety and productivity, but improved manipulator arm designs and controls are needed.

A study of various alternative joint torque control schemes for the planar motion of two pinned flexible beams has been conducted. This type of system is displayed schematically in Fig. 1. The immediate application for the results is in the area of manipulator arms and this application flavors the analysis. The specific results are of interest outside this area since many beam-like components are found in mechanical hardware. The techniques used to analyze these distributed flexible systems are of even more general interest.

Manipulator arms require a reasonable accuracy in response of the arm's end point to input commands to the joint contro system. This accuracy is deteriorated by structural deformation especially when the deformation is oscillatory. The simplest way to eliminate these vibrations is to increase the rigidity of the arm, which ultimately means increasing the load bearing material. Adverse effects of this practice have been increased torque and power requirements, higher feedback gains, higher total system weight, and a typical payload capacity of 10 percent of the arm weight [16].[2] Thus in the interest of better arm design one would like to understand the limitations imposed by the structure on arm performance. These limitations are intimately related to the type of control scheme used and can be overcome to some extent by recognizing the flexible nature of the arm structure when establishing the control scheme and its parameters.

Characterization of the Problem

This study was conducted to yield practical design information and yet recognize the essential distributed nature of the manipulator structure. Prior results [5, 6, 9, 14, 15] in optimal control of distributed systems are largely for systems defined by a single set of partial differential equations, instead of two interacting sets as is the case here.

The systems studied here include distributed beams considered to be adequately modeled by the Bernoulli-Euler beam equations. Control torque is applied at hinged joints between the beams and between the inboard or proximal beam and an inertial ground. Lumped masses at the distal end of each beam representing

[1]This work was supported by NASA Marshall Space Flight Center under contract NAS8-28055 to the Department of Mechanical Engineering, Massachusetts Institute of Technology, and by Fundacao de Amparo a Pesquisa do Estado de Sao Paulo, Brazil.

Contributed by the Automatic Control Division for presentation at the Winter Annual Meeting, Houston, Texas, November 30-December 5, 1975, of THE AMERICAN SOCIETY OF MECHANICAL ENGINEERS. Manuscript received at ASME Headquarters, July 23, 1975. Paper No. 75-WA/Aut-26.

Copies will be available until August, 1976.

[2]Numbers in brackets designate References at end of paper.

Discussion on this paper will be accepted at ASME Headquarters until January 5, 1976

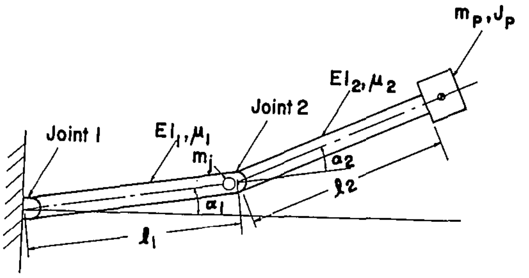

Fig. 1 Schematic system and nomenclature

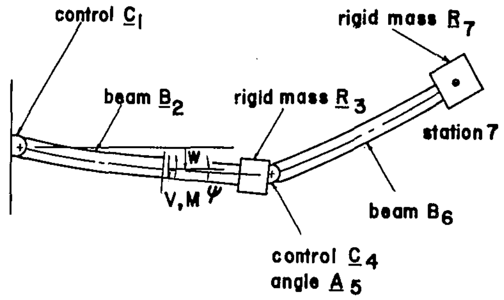

$$\underline{z}_0 = \underline{C}_1 \underline{B}_2 \underline{R}_3 \underline{C}_4 \underline{A}_5 \underline{B}_6 \underline{R}_7 \underline{z}_7 = \underline{U}\, \underline{z}_7$$

$$\begin{bmatrix} -W \\ \psi \\ M \\ V \end{bmatrix} = \begin{bmatrix} -\text{displacement} \\ \text{angle} \\ \text{moment} \\ \text{shear force} \end{bmatrix}$$

Fig. 2 Transfer matrix representation and state variables

actuator and payload mass are considered. A feedback control law is desired which commands torque on the basis of feedback which could be measured at or observed from measurements at discrete points. The control system serves the purpose of tracking desired trajectories as well as regulating the system position in the face of disturbance loadings.

The position of the dominant system poles was the major consideration when judging the relative merit of competing arm systems. Large eigenvalue absolute value with "adequate" damping is indicative of high arm bandwidth which is necessary for manipulators capable of fast accurate small motions. Higher modes were required to remain stable and time responses obtained from both linear and nonlinear models were used to further check the system behavior.

System Models Used

Two complimentary models were employed in this study. One is basically a time domain model employing truncation of a modal description of the beam shapes and allows nonlinear effects to be included in the system simulation. The other is a frequency domain technique which requires linear assumptions including small motions about an equilibrium position with no Coriolis, centrifugal or gravity forces, but it can easily describe various beam configurations and includes distributed effects with no modal truncation. The two models agree very well in those situations where comparable results could be obtained and accurately predict experimental results obtained.

A. Frequency Domain Model. The frequency domain model of the arm was implemented via the transfer matrix methods which have found frequent use in applied mechanics but only rarely for purposes of control. With the use of numerical techniques the frequency domain model becomes a versatile design tool.

Transfer Matrix Formulation. The transfer matrix (t.m.) state variables[3] chosen for description of the arm are those used by Pestel and Leckie [11] for representing the flexural vibrations of a beam, and are displayed in Fig. 2. Because slender beams are vastly more rigid in compression than in flexure, four t.m. state variables adequately describe the general planar motion of an arm system. A transfer matrix for various arm model elements such as controlled joints, joint angles, Bernoulli-Euler beams, and rigid inertias can be constructed. These matrices relate the Laplace transform of the t.m. state variables at one of the two stations of the elements to the Laplace transform of the t.m. state variables at the other station. The product of several transfer matrices constitutes a complete description of those elements clamped consecutively together since the t.m. state variables are identical at the common station of two elements. Fig. 2 displays a possible arm and its transfer matrix implementation.

By imposing boundary conditions at either end of the arm model one specifies some of the t.m. state variables related by the product matrix.

The controlled joint transfer matrix relates the t.m. state vectors at stations i and $i + 1$ as follows:

$$\mathbf{z}_i = \begin{bmatrix} -w \\ \psi \\ M \\ V \end{bmatrix}_i = \begin{bmatrix} 1 & 0 & 0 & 0 \\ 0 & 1 & 1/k(s) & 0 \\ 0 & 0 & 1 & 0 \\ 0 & 0 & 0 & 1 \end{bmatrix} \begin{bmatrix} -w \\ \psi \\ M \\ V \end{bmatrix}_{i+1} = \mathbf{C}\mathbf{z}_{i+1} \quad (1)$$

where

$$k(s) = \frac{M_{i+1}}{\psi_i - \psi_{i+1}} = \frac{M_i}{\psi_i - \psi_{i+1}}$$

s = the Laplace variable

$k(s)$ = the transfer function which relates the joint angle to the control torque applied.

The only work which will be presented here using the transfer matrix model is for k of the form

$$k(s) = k_p + sk_v \quad (2)$$

That is, control torque equal to the sum of the joint angle and its derivative, each times appropriate gains.

Numerical Techniques in Implementation. The transfer matrices of some elements, especially distributed beams, are reasonably complex and are best evaluated by digital computer. The matrix product is then taken numerically and numerical techniques are necessary to extract useful information from the model. The first step in obtaining useful information from the matrix relation of the model equation (3).

$$\mathbf{z}_0 = \mathbf{U}(s)\mathbf{z}_n \quad (3)$$

is to constrain certain of the t.m. state variables and thus provide system boundary conditions.

If the four constrained t.m. state variables are all zero one can find in equation (3) two homogeneous equations linear in two t.m. state variables at station n. The determinant of the coefficients (which are a function of the complex variable s)

[3] The term transfer matrix variables (abbreviated "t.m. state variables") is used to avoid confusion with state variables involved in a state variable formulation of modern control theory.

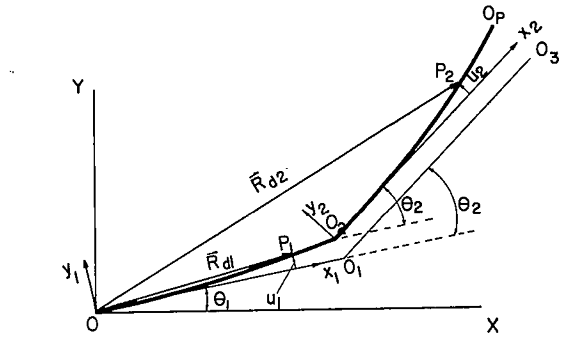

Fig. 3 Coordinate systems in the time domain model

must equal zero for a nontrivial solution. The values of s at which this condition is satisfied are the eigenvalues of the system. The present work utilized two dimensional numerical searches over the complex plane to find the eigenvalues from this relation.

If one or more of the constrained t.m. state variables are pure sinusoids of constant amplitude and a single frequency ω the steady-state forced frequency response can be found. Equation (3) is evaluated with $s = j\omega$ and with the constrained t.m. state variables equal to the complex amplitude of the sinusoidal forcing function. From these samples of the frequency response the time response can be calculated via the fast Fourier transform algorithm of Cooley and Tukey [1]. Details of this implementation are found in [2].

B. Time Domain Model. The derivation of the time domain model is based on the description of the system in Fig. 3. In order to describe the motions, three reference frames and their unit vectors [4] can be defined:

$[0XY]$ an inertial reference frame with origin at joint 1 and unit vector $\{\mathbf{U}\}$

$[0x_1y_1]$ a reference frame with origin at 0, axis x_1 tangent to beam 1 at point 0 and unit vector $\{\mathbf{U}_1\}$

$[0_2x_2y_2]$ a reference frame with origin at joint 2, with axis x_2 tangent to beam 2 at point 0_2, and unit vector $\{\mathbf{U}_2\}$. The unit vectors can be related by rotation matrices C_1 and C_2 as follows:

$$\{\mathbf{U}_1\} = [C_1]\{\mathbf{U}\}\ ,\ \{\mathbf{U}_2\} = [C_2]\{\mathbf{U}\}$$

Also, the two angles can be defined:

$\theta_1(t)$ is the angle between the axes x_1 and X

$\theta_2(t)$ is the angle between the axes x_1 and x_2

If now a new system is defined as being formed by two segments 00_1 and 0_10_3 having the angle θ_2 at 0_1, the overall motion can be understood as a motion of a hypothetical rigid system $[0\ 0_1\ 0_3]$ and a flexible motion of the beams 1 and 2 with respect to this moving system.

Kinematic Description. As indicated in Fig. 3, any point P_i can be specified if a new variable $u_i(x_i, t)$ is defined as being the coordinate of the flexible motion with respect to the reference frame $[0x_iy_i]$. The vector position of point P_i would be:

$$\mathbf{R}_{di} = x_i\mathbf{u}_{xi} + y_i\mathbf{u}_{yi} = \{\mathbf{U}_i\}^t \begin{Bmatrix} x_i \\ y_i \end{Bmatrix}$$

The vector position of any point in beam 1 is

$$\mathbf{R}_{d1} = \{\mathbf{U}_1\}^t \begin{Bmatrix} x_1 \\ u_1 \end{Bmatrix} = \{\mathbf{U}\}^t[C_1]^t \begin{Bmatrix} x_1 \\ u_1 \end{Bmatrix}$$

Assuming small deflections one can consider the paths of points 0_1 and 0_p as straight lines normal to the respective reference frames. Then, as shown in Fig. 3, the vector position of any point P_2 on beam 2 will be

$$\mathbf{R}_{d2} = \mathbf{00}_1 + \mathbf{0}_1\mathbf{0}_2 + \mathbf{0}_2\mathbf{P}_2$$

If now

u_{1E} = flexible displacement at end of beam 1

l_1 = length of beam 1

l_2 = length of beam 2

$$\mathbf{R}_{d2} = \{\mathbf{U}\}^t \cdot \left[\begin{Bmatrix} l_1c\theta_1 \\ l_1s\theta_1 \end{Bmatrix} + \begin{Bmatrix} -u_{1E}s\theta_1 \\ u_{1E}c\theta_1 \end{Bmatrix} + [C_1]^t \begin{Bmatrix} x_2 \\ 0 \end{Bmatrix} + [C_2]^t \begin{Bmatrix} 0 \\ u_2 \end{Bmatrix} \right] \tag{5}$$

where $c\theta = \cos\theta$ and $s\theta = \sin\theta$.

These position vectors can be differentiated with respect to time to obtain $\dot{\mathbf{R}}_{d1}$ and $\dot{\mathbf{R}}_{d2}$, the velocity vectors. For any mass m_j concentrated at joint 2 the position $\mathbf{R}_j$ and velocity $\dot{\mathbf{R}}_j$ will be the same as for the end of beam 1 and for any payload of mass m_p and moment of inertia about its center of gravity J_p the position $\mathbf{R}_p$ and velocity will be the same as for the end of beam 2. This result can be used to write the total system kinetic energy:

$$T = \frac{1}{2}\int_{m_1} \dot{\mathbf{R}}_{d1}\cdot\dot{\mathbf{R}}_{d1}dm + \frac{1}{2}\int_{m2} \dot{\mathbf{R}}_{d2}\cdot\dot{\mathbf{R}}_{d2}dm + \frac{1}{2}m_j\dot{\mathbf{R}}_j\cdot\dot{\mathbf{R}}_j + \frac{1}{2}m_p\dot{\mathbf{R}}_p\cdot\dot{\mathbf{R}}_p + \frac{1}{2}J_p\left(\frac{\partial\dot{u}_2}{\partial x_2}\bigg|_{x_2=l_2}\right)^2 \tag{6}$$

The potential energy of the system is assumed to be composed of the energy associated with the rigid motion plus the elastic potential energy of the beams. Assuming $0X$ as the reference position, the total potential of the system for small u_1 and u_2 can be approximated by

$$V = m_1gl_1(1 - c\theta_1)/2 + m_jgl_1(1 - c\theta_1) + m_2g\left[l_1(1 - c\theta_1) + \frac{l_2}{2}(1 - c(\theta_1 + \theta_2))\right]/2 + m_pg[l_1(1 - c\theta_1) + l_2(1 - c(\theta_1 + \theta_2))] - \frac{1}{2}\int_0^{l_1} E_1I_1\left(\frac{\partial^2u_1}{\partial x_1^2}\right)^2 dx - \frac{1}{2}\int_0^{l_2} E_2I_2\left(\frac{\partial^2u_2}{\partial x_2^2}\right)^2 dx \tag{7}$$

where g is the component of gravity acceleration in the $0X$ direction. E_1I_1, and E_2I_2 are the stiffnesses of links 1 and 2, respectively, assumed constant for the purpose of this model.

In order to write the equations of motion of the system the method of assumed modes [8] is used. A solution of the flexible motions is assumed to be a linear combination of admissible functions $\Phi_{ij}(x_i)$ (which satisfies the essential boundary conditions [3] for the reference frame used) multiplied by time dependent generalized coordinates $q_{ij}(t)$. Thus the flexible motion is written as

$$u_1 = \sum_{i=1}^{n} \Phi_{1i}(x_1)q_{1i}(t)$$
$$u_2 = \sum_{i=1}^{n} \Phi_{2i}(x_2)q_{2i}(t) \tag{8}$$

Assuming that the amplitude of the higher modes of the flexible links are very small compared with the first ones, the system can be truncated with n equal 2, resulting in a six degree-of-freedom problem. If the $\Phi_{ij}(x)$, $i = 1, 2$ are assumed to be the eigenfunctions of a clamped free beam the essential boundary conditions will be satisfied and the integrals in equations (6) and (7) can be evaluated. Lagrange's equations yield the system equations which when linearized are of the from

$$\dot{\mathbf{q}} = \mathbf{A}\mathbf{q} + \mathbf{B}\mathbf{u} \tag{9}$$

where

$\mathbf{q} = [\theta_1\ \theta_2\ q_{11}\ q_{12}\ q_{21}\ q_{22}\ \dot{\theta}_1\ \dot{\theta}_2\ \dot{q}_{11}\ \dot{q}_{12}\ \dot{q}_{21}\ \dot{q}_{22}]^T$

$\mathbf{A}$ = the system plant matrix for given nominal joint angles

$\mathbf{B}$ = the system control matrix for given nominal joint angles

$\mathbf{u}$ = a 2×1 control vector of torques

Details of development and the equations of motion are to be found in reference [7].

Control Schemes Studied

Three basic control configurations were studied. Two are based on the concept of a rigid system. The third incorporates feedback of the flexible state variables. All three configurations are linear feedback schemes.

A. Feedback Based on Rigid Assumptions. These control configurations utilize only joint angle and angular velocity measurements and are most practical to implement. They are based on a rigid model of the arm but have been applied to the flexible models to determine the limitations imposed by the flexibility.

Rigid Arm Model. The rigid arm is essentially a double pendulum with system equations given by:

$$\mathbf{J}\ddot{\boldsymbol{\alpha}} = \mathbf{B}\boldsymbol{\tau}$$

$\mathbf{J}$ = a 2 by 2 inertia matrix

$$\boldsymbol{\alpha} = \begin{bmatrix} \alpha_1 \\ \alpha_2 \end{bmatrix} = \begin{bmatrix} \text{angle of link 1 with respect to an inertial reference} \\ \text{angle between the axes of link 1 and 2} \end{bmatrix}$$

$$\boldsymbol{\tau} = \begin{bmatrix} \tau_1 \\ \tau_2 \end{bmatrix} = \text{torques applied at joints 1 and 2}$$

$\mathbf{B}$ = a 2 by 2 matrix relating the effects of the control torques.

The desired feedback control law would ralate $\boldsymbol{\tau}$ to $\boldsymbol{\alpha}$ and $\dot{\boldsymbol{\alpha}}$ resulting in the state variable form of equation (10).

$$\begin{bmatrix} \dot{\alpha} \\ \ddot{\alpha} \end{bmatrix} = \begin{bmatrix} \mathbf{0} & \mathbf{I} \\ \mathbf{J}^{-1}\mathbf{BK} & \mathbf{J}^{-1}\mathbf{BC} \end{bmatrix} \begin{bmatrix} \alpha \\ \dot{\alpha} \end{bmatrix} \tag{10}$$

$\mathbf{K}$ = a 2 by 2 matrix of joint angle position feedback gains

$\mathbf{C}$ = a 2 by 2 matrix of joint angular velocity feedback gains

$\mathbf{J}^{-1}$ will exist for any physical system

The simplest type of control results in diagonal matrices $\mathbf{K}$ and $\mathbf{C}$. Thus each joint is controlled independently using measurements on that joint. This type of control will be termed independent joint control (IJC) and is widely found in practice. It is explored below using the frequency domain model.

The general case where K and C are not diagonal is referred to as general rigid control (GRC). It can result in improved performance with a slight increase in complexity. It is explored below using the time domain model.

With IJC it is feasible to explore system performance by varying all four gains independently and finding values which yield good relative pole locations in either the flexible or the rigid model. Sufficient design freedom does not exist for arbitrary specification of the poles.

With GRC a total of eight gains enables one to arbitrarily specify the eigenvalues of the rigid model. One way to do this in the special case of rigid arms is to select the gains such that

$$\mathbf{J}^{-1}\mathbf{BK} = \begin{bmatrix} -\omega_1^2 & 0 \\ 0 & -\omega_2^2 \end{bmatrix}$$

$$\mathbf{J}^{-1}\mathbf{BC} = \begin{bmatrix} -2\zeta_1\omega_1 & 0 \\ 0 & -2\zeta_2\omega_2 \end{bmatrix} \tag{11}$$

where ω_1, ω_2 are the desired eigenvalue magnitudes and ζ_1, ζ_2 are the corresponding damping ratios. This method was suggested for use in manipulator control by Whitney in [10].

B. Feedback of Flexible State Variables. Using the linearized time domain model equations in state variable form as expressed in equation (9) one can propose linear feedback of the flexible system state variables. This control scheme is referred to as flexible feedback control (FFC). Control is given by a feedback law

$$\mathbf{u} = \mathbf{F}\mathbf{q} \tag{12}$$

where $\mathbf{F}$ is a 2×12 matrix of feedback gains. It will be recalled from the formulation of (9) and Fig. 3 that of the 12 state variables in $\mathbf{q}$ only θ_1 and $\dot{\theta}_1$ can be conveniently measured using common instrumentation such as potentiometers or tachometers. The values of θ_2 and $\dot{\theta}_2$ in $\mathbf{q}$ differ from the joint angle and velocity only by the rotation of the end of the first beam. The contribution of the two modal coordinates of each beam cannot be determined directly by simple measurements but might be determined from an observer, or inferred from measurements of the beam deflection. This has not been done in the present work but the control configuration has been explored based on perfect information of the state variables.

The matrix F has a total of 24 elements which must be specified. Such an undertaking must be approached systematically to obtain desired pole locations and two methods have been used. The first of these is a pole shifting algorithm developed by Simon [12, 13] and implemented by Maizza-Neto [7]. The reader is referred to those works for specific details. The effect of the algorithm is to prescribe the gains required to move a subset of the poles to new locations while maintaining the remaining poles in the same position.

As implemented by Maizza-Neto the non-uniqueness of the gains is resolved by assuming a fixed ratio of feedback gains in the two gain vectors required to shift two poles. This ratio is ± 1 depending on the signs of the terms in the mode controllability matrix.

The second method for selecting gains with FFC is based on the sensitivity of the location of the various poles to changes in the various gains. By observing the sensitivity of the dominant poles one can adjust the gains to improve the pole position. Caution must be observed that higher modes are not driven into the right half plane. The adjustment procedure is tedious because sensitivity is strongly dependent on the pole position and only small variations in gains can be made with the results accurately predicted by the sensitivities. Details of this procedure are also found in [7].

Results

Results have been obtained for the control schemes described for various values of the nondimensionalized parameters of the system. A representative sample of the results is all that space will allow. The relative merit of the various control schemes and the limitations imposed on their performance by the system flexibility is evidenced by the results that have been obtained.

A. Nondimensionalization. Through nondimensionalization a

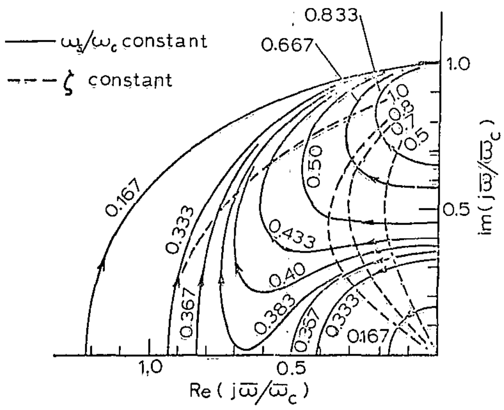

Fig. 4 Complex eigenvalues for IJC at joint 2, joint 1 locked

reduction in the total number of system parameters and a more general understanding of distributed beam systems can be obtained. This also avoids numerical problems in the calculations in some cases. The nondimensionalization in this presentation is with respect to the physical quantities expressed in Table 1 and displayed in Fig. 1.

Table 1 Primary variables for nondimensionalization

Physical quantity	symbol	dimension
Stiffness of beam 1	EI_1	FL^2
Total arm length	l	L
Average beam mass per unit length	μ	ML^{-1}

where $l = l_1 + l_2$

$$\mu = \frac{\mu_1 l_1 + \mu_2 l_2}{l_1 + l_2}$$

μ_1, μ_2 = mass density/unit length of beam 1, 2

l_1, l_2 = length of beam 1, 2

E = Young's modulus

I_1 = Cross section area moment of inertia

$= r_1^4(1 - k_r^4)/4$

r_1 = outer radius of beam 1

k_r = geometric factor which, for a concentric circular cross section, corresponds to (inner radius)/(outer radius).

The parameters in Table 1 can be combined to yield any product of the basic dimensions, F, L, and M for nondimensionalizing the parameters of the system. In addition the dimension T can be obtained as

$$t_d = \frac{\mu l^3}{EI_1}, \quad \omega_d = \frac{1}{t_d} = \sqrt{\frac{EI_1}{\mu l^3}}$$

The nondimensional value of a parameter will be designated with a bar, for example for a frequency $\omega = -js$

$$\bar{\omega} = \omega/\omega_d$$

For all the results displayed here,

$$l_1 = l_2, \text{ i.e. } \bar{l}_1 = \bar{l}_2 = 0.5$$

The nondimensional stiffness of beam 2, $\bar{E}I_2 = EI_2/EI_1$ is one of the important design parameters which, with the nondimensional payload mass $\bar{m}_p$, affects the arm bandwidth obtainable. For $\bar{m}_p = 0$ the selection of $\bar{E}I_2$ less than one appreciably raises the bandwidth obtainable, while for $\bar{m}_p = 1$ this does not seem to be the case. The value of $\bar{E}I_2$ used in the results should be noted.

B. Dominant Eigenvalue Locations for IJC and GRC. The desire for higher arm bandwidth has been characterized as a desire for dominant eigenvalues of larger magnitude and "adequate" damping. Damping ratios from 0.6 to 1.0 are generally acceptable for arm systems where overshoot is penalized and can be hazardous. When designing a control for an essentially rigid arm the dominant complex conjugate poles would be placed in this region. In order to increase the arm bandwidth the magnitude of these eigenvalues is increased until the rigid assumption becomes poor. The most severe flexible effect on the rigid control schemes IJC and GRC is the deterioration of damping on the dominant pole pair.

IJC Root Loci. The simple IJC results are best introduced by clamping joint 1 rigidly to ground. This is equivalent to increasing without limit the angular position feedback of joint 1. The rigid beam model of this case is described by a second order system with conjugate eigenvalues of magnitude ω_s and damping ratio ζ. This reduced form of IJC control can be studied by varying the nondimensional form of the parameters $\bar{\omega}_s$ and $\bar{\zeta} = \zeta$. The result of these variations on the flexible model is shown in Fig. 4 for the simple case of $m_p = 0$, $\alpha_2 = 0$, (Fig. 1) and equal beams. For small values of $\bar{\omega}_s$ and for $\zeta < 1.0$ the root loci is indistinguishable from a rigid second order system. For high values of $\bar{\omega}_s$ this deviates drastically and as ζ is increased from 0 the actual complex pole pair of the flexible system reaches a maximum damping, then returns toward the imaginary axis. Corresponding to this motion of the complex pair a real root moves in from the negative real axis toward the origin and for $\zeta > 1.0$ the system is no longer adequately described by the complex pair alone. The maximum value of the dominant eigenvalue at which adequate damping can be achieved depends on the relative stiffness and mass of beams 1 and 2, the payload mass, and on the angle of joint 2. The critical value seems in a wide variety of cases to be approximately one-half of $\bar{\omega}_c$, the natural frequency of the arm with both joints clamped.

For two joints controlled with IJC the rigid design procedure is less straightforward and arbitrary pole placement cannot be achieved. An acceptable relative pole pattern is obtained for

$$k_1 = 50\, k_2\mu_1/\mu_2$$

$$c_1 = 10\, k_2\mu_1/(p\mu_2)$$

$$c_2 = 1.17\, k_2/p$$

where k_1, k_2 are angular position feedback gains of joints 1 and 2 respectively and c_1, c_2 are angular velocity feedback gains of joints 1 and 2, respectively.

$$p = \sqrt{\frac{k_2}{\mu l_2^3/3 + m_p l_2^2}} \qquad [T^{-1}]$$

Fig. 5 displays for equal beams, no payload and, $\alpha_2 = 0$ the two most dominant eigenvalues as the parameter $\bar{p}$ is increased, increasing system bandwidth. Once again $\bar{\omega}_c/2$ is an approximate limit for the bandwidth of this flexible system and for other systems of this type using IJC.

IJC is inherently stable in all cases, since the system could be realized with strictly passive components. Impulse responses obtained from inverse transforming the frequency response show very little effect of the higher system modes. More detailed consideration of this control scheme is found in [2].

GRC Root Loci. The simple IJC control has been characterized as limited to approximately $\bar{\omega}_c/2$ by system flexibility. The more complicated forms of control should demonstrate some improvement to justify their increased complexity. GRC gains for Fig. 6 were determined from equation (11) for $\omega_1 = \omega_2$ and $\zeta_1 = \zeta_2$. It was found for $\omega_1 \neq \omega_2$ that the deterioration of damping on

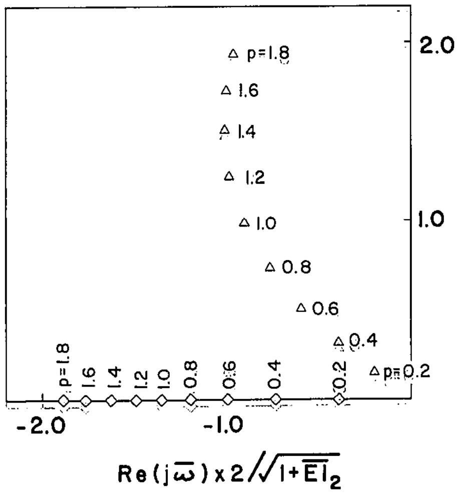

Fig. 5 Dominant eigenvalues at IJC attempts higher bandwidth. $\overline{EI}_2 = 1.0$, $\alpha = 0$, $\overline{m}_p = 0$

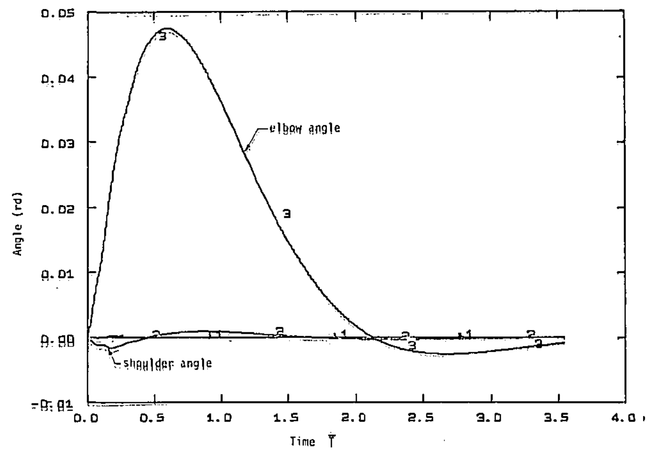

Fig. 7(a) Angle response to torque impulse at joint 2 for GRC. $\overline{EI}_2 = 0.1667$, $\alpha_2 = 0$, $\overline{m}_p = 0$

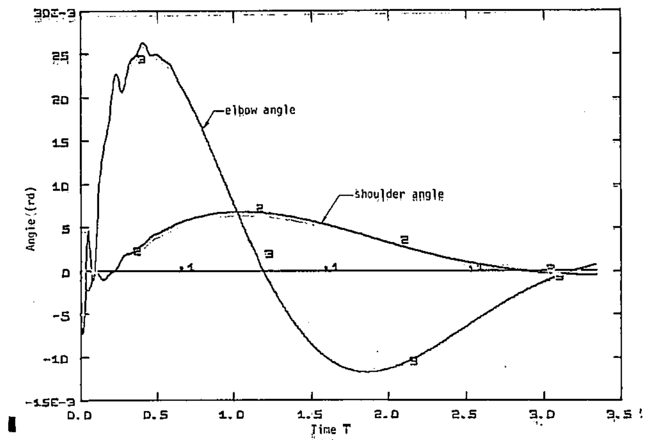

Fig. 7(b) Angle response to torque impulse at joint 2 for FFC. $\overline{EI}_2 = 0.1667$, $\alpha_2 = 0$, $\overline{m}_p = 0.$

the dominant eigenvalue occurred at lower eigenvalue magnitudes and that in some cases the higher modes were unstable. As Fig. 6 indicates in comparison with Fig. 5 an improvement of 100 percent in the maximum arm bandwidth permitted by the flexible arm structure can be achieved by including the cross joint gains. This is of course variable with payload mass and relative masses and stiffnesses of the beams, but eigenvalues with magnitude on the order of the clamped natural frequency can be achieved. It should be mentioned that this result is obtained using a rigid design procedure, and gain adjustments based on the sensitivity of the poles may yield improvement. Efforts to date using sensitivities have been discouraging, however.

C. Results Using FFC and the Simon Mitter Algorithm. The Simon Mitter algorithm [12, 13] as implemented by Maizza-Neto was used to determine the gains for the matrix **F** of feedback gains as described in equation (12). The eigenvalues of the flexible model could be moved in an arbitrary manner by the algorithm with practical limitations arising due to the sensitivities of the eigenvalues to perturbations of the system parameters, including feedback gains and joint angles. Due to these practical limitations it is not possible to conclude that this control configuration and design method will result in superior performance, especially in application to manipulator arms.

Fig. 7(a) and (b) compares GRC to FFC based on time responses from torque impulses at joint 2. The eigenvalues requested from the Simon Mitter algorithm were identical but the responses of Fig. 7 are markedly different. This results from different methods of resloving the nonuniqueness of the gains. The gains are completely different as are the eigenvectors. The lower torque requirements observed for GRC in Fig. 8 favor that

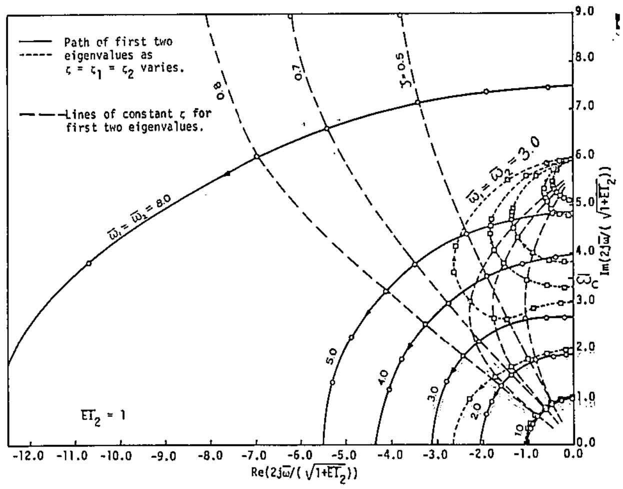

Fig. 6 Dominant eigenvalues as GRC attempts higher bandwidth. $\overline{EI}_2 = 1.0$, $\alpha_2 = 0°$, $\overline{m}_p = 0$

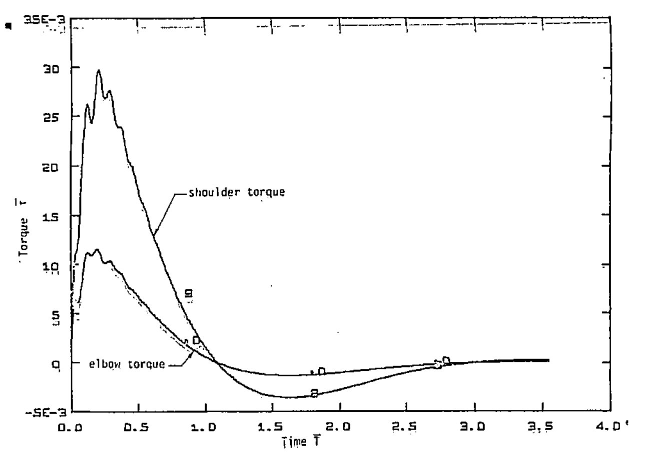

Fig. 8(a) Torque response to torque impulse at joint 2 for GRC. $\overline{EI}_2 = 0.1667$, $\alpha_2 = 0$, $m_p = 0.$

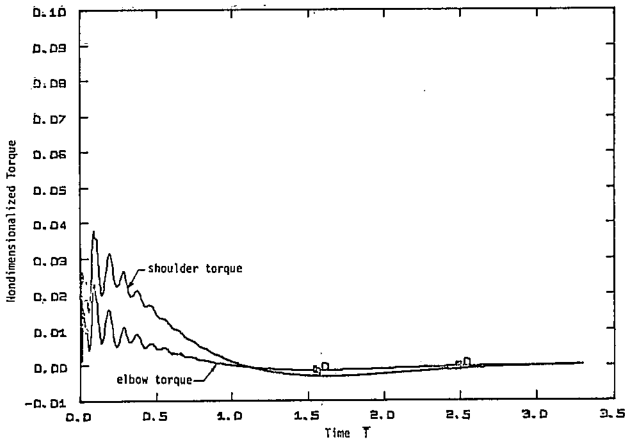

Fig. 8(*b*) Torque response to torque impulse at joint 2 with FFC. $\overline{EI}_2$ = 0.1667, α_2 = 0, $\overline{m}_p$ = 0.

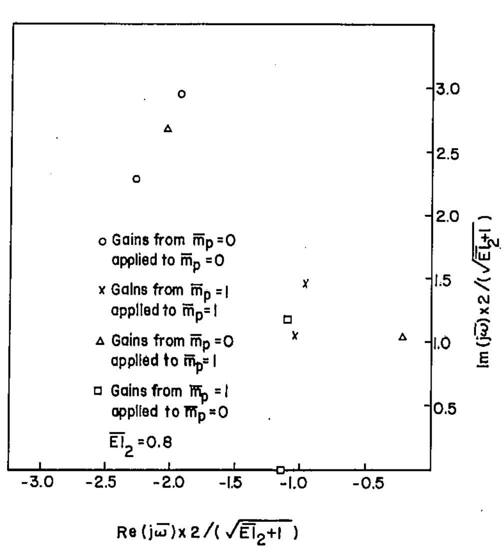

Fig. 9 Dominant eigenvalues for constant GRC gains with changes in payload. $\overline{EI}_2$ = 0.8, α_2 = 0.

scheme over FFC.

Table 2 indicates another disadvantage of modal control for the application at hand. Listed there are the eigenvalues after joint 2 has moved from the design point of 0° to 90°. Certain of the higher poles show positive real parts indicating instability. GRC eigenvalues for the same angle change remain stable.

In some cases modal control may be useful if the system is constant and accurately known, but for manipulator application this tends not to be the case.

D. Arm Operation With Constant GRC Gains. The normal operation of a manipulator arm results in large joint angle and payload changes. These changes in the system change eigenvalues and arm dynamics. It is desireable to maintain constant gains for system simplicity if the resulting performance is acceptable. Fig. 9 displays the shift in arm eigenvalues when the design payload of m_p has been removed. Also displayed are the eigenvalues which could be obtained if the gains were adjusted to account for the altered system. These results indicate that constant gains, if used, should correspond to the case where the arm carries a payload.

The variation of dominant roots for joint 2 varying from 0 deg to 90 deg are shown in Fig. 10 indicating some deterioration in the damping ratio of one of the two dominant pole pairs.

Table 2 Eigenvalues of flexible model $\overline{EI}_2$ = 0.1667, $\overline{m}_p$ = 0

GRC $\alpha_2 = 0$		FFC $\alpha_2 = 0$		FFC $\alpha_2 = \pi/2$ (designed for $\alpha_2 = 0$)	
REAL	IMAG.	REAL	IMAG.	REAL	IMAG.
−1.4130	±1.4522	−1.3309	±1.4407	−0.4136	±0.9630
−1.3817	±1.6114	−1.4138	±1.6263	−2.2831	±1.6225
−11.167	0.0000	−11.847	0.0000	−30.070	0.0000
−5.9610	±33.406	−6.0627	±33.458	−18.631	±30.300
−5.6658	±68.974	−5.8295	±67.830	0.2469	±43.797
−55.790	±103.55	−54.836	±103.54	−42.319	±96.351
−489.59	0.0000	−482.15	0.0000	−375.39	0.0000

Conclusions

Two useful procedures have been presented for modeling the planar motion of hinged flexible beams with controlled joints. One procedure incorporates transfer matrices and numerical techniques to derive useful information from the frequency domain model. The other procedure incorporates a truncated modal description of dynamic beam flexure. The flexible and "rigid" components of the position are used to write Lagrange's equation for the system, and thus the approximate equations of motion are derived.

The models derived were used to explore three control schemes. GRC and IJC were based on the joint angle measurements with and without interjoint feedback, respectively. FFC feeds back the flexible modes of the beam as well. IJC is limited in the bandwidth it can provide to approximately $\bar{\omega}_c/2$ by inadequate damping. GRC shows marked improvement with a slight increase in complexity providing bandwidth as high as $\bar{\omega}_c$. FFC as implemented showed high sensitivities to parameter perturbations and somewhat higher torque requirements, and requires much more complexity, severely detracting from its usefulness for manipulators.

References

1 Bergland, G. D., "A Guided Tour of the Fast-Fourier Transform," *IEEE Spectrum*, July 1969.

2 Book, Wayne, J., "Modeling Design and Control of Flexible Manipulator Arms," PhD thesis, Dept. of Mechanical Engineering, Massachusetts Institute of Technology, 1974.

3 Crandall, S. H., *Engineering Analysis*, McGraw-Hill, 1956.

4 Crandall, S. H., Karnopp, D. C., Kirtz, E., and Pridmore-Brown, D. C., *Dynamics of Mechanical and Electromechanical Systems*, McGraw-Hill, 1968.

5 Koehne, Manfred, "Optimal Feedback Control of Flexible Mechanical Systems," Proceedings of IFAC *Symposium on the Optimal Control of Distributed Parameter Systems*, Banf, Canada, 1971.

6 Komkov, Vadim, *Optimal Control Theory for the Damping of Vibration of Simple Elastic Systems*, Lecture Notes in Mathematics, No. 253, Springer-Verlag, 1972.

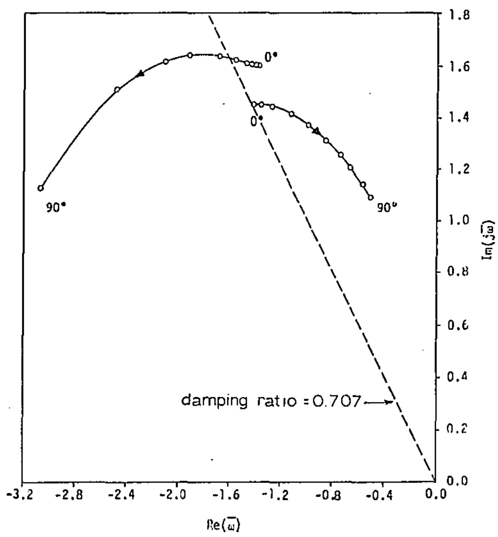

Fig. 10 Dominant eigenvalues for constant GRC gains with changes in α_2. $\overline{El_2}$ = 0.1667m m_p = 0.

7 Maizza-Neto, Octavio, "Modal Analysis and Control of Flexible Manipulator Arms," PhD thesis, Dept. of Mechanical Engineering, Massachusetts Institute of Technology, 1974.

8 Meirovitch, L., *Analytical Methods in Vibrations*, The MacMillian Co., 1967.

9 Mirro, John, "Automatic Feedback Control of a Vibrating Flexible Beam," MS thesis, Dept. of Mechanical Engineering, Massachusetts Institute of Technology, Aug. 1972.

10 Nevins, J. L., Whitney, D. E., and Simunovic, S. N., "Report on Advanced Automation, System Architecture for Assembly Machines," Charles Stark Draper Laboratory Report, R 764, Nov. 1973.

11 Pestel, Eduard C., and Leckie, Frederick A., *Matrix Methods in Elasto-Mechanics*, McGraw-Hill, 1963.

12 Simon, J. D., "Theory and Application of Modal Control," PhD thesis, Case Institute of Technology, 1967.

13 Simon, J. D., and Mitter, S. K., "A Theory of Modal Control," *Information and Control*, Vol. 13, Oct. 1968, pp. 316–353.

14 Van de Vegte, J., Optimal and Constrained-Optimal Controls for Vibrating Beams," JACC Paper 19-C, 1970, p. 469.

15 Vaughan, D. R., "Application of Distributed Parameter Concepts to Dynamic Analysis and Control of Bending Vibrations," *Journal of Basic Engineering*, Trans. ASME, Series D, Vol. 90, No. 2, p. 157.

16 Whitney, D. E., Book, W. J., Lynch, P. M., "Design and Control Considerations for Industrial and Space Manipulators," JACC, 1974.

Printed in U.S.A.